

Electrodeposited Ru Nanoparticles for Electrochemical Reduction of NAD⁺ to NADH

Gul Rahman^{1,2}, Ji yeon Lim¹, Kwang- Deog Jung¹, Oh-Shim Joo^{1,*}

¹ Clean Energy Research Center, Korea Institute of Science and Technology (KIST), Seongbuk-gu, Seoul 130-650, Republic of Korea

² School of Science, University of Science and Technology, 52 Eoeun dong, Yuseong-gu, Daejeon 305-333, Republic of Korea

*E-mail: jooat61@gmail.com

Received: 29 March 2011 / Accepted: 30 May 2011 / Published: 1 July 2011

Ruthenium nanoparticles (RuNP) were deposited on glassy carbon (GC) substrate by cathodic electrodeposition method. The electrocatalytic properties of RuNP deposits were characterized by scanning electron microscopy, cyclic voltammetry and linear sweep voltammetry. Results of these studies showed that very small sized RuNP are deposited with significantly large particle density which is attributed to the controlled deposition potential. The resulted RuNP/GC electrodes showed remarkable catalytic activity for electrochemical reduction of NAD⁺ to NADH, indicating its potential for electrocatalytic applications.

Keywords: Glassy carbon (GC); Electrodeposition; Ruthenium nanoparticles (RuNP); NAD⁺ reduction

1. INTRODUCTION

Ruthenium nanoparticles (RuNP) have attracted considerable scientific attention as they have remarkable size dependant properties [1, 2]. They have been extensively used for practical applications in many fields such as catalysis, biosensors, capacitors and electrochemical reactions [3-5]. Great attention has been given to RuNP due to their catalytic activity towards electrochemical hydrogenation of NAD⁺ (β - Nicotinamide adenine dinucleotide monohydrate) to NADH (nicotinamide adenine dinucleotide) [6]. NADH is a cofactor that plays a crucial role in most of the biochemical reactions catalyzed by redox enzymes. Its reduced and enzymatically active form (1, 4-NADH), shuttles two electrons and a proton to the substrate in the presence of appropriate enzyme to form NAD⁺. The use of

the cofactor, however, is limited by its high cost that has been the major motivation for research in the development of NADH regeneration [7].

The properties of metal nanoparticles are dominated by several factors such as size and size distribution, structure of particle, shape of particle and particle density. In turn, these parameters strongly depend on synthetic control, preparation method and stability of the particles. The main problem in the preparation of ruthenium nanoparticles is the agglomeration which results in the formation of large-sized particles. Different approaches have been utilized to control the size, shape and morphology of RuNP. The use of polymer and ligand as capping agent has been considerably addressed in the past few years to inhibit the particles from coalescing and allow them to form various shapes [8, 9].

J.Y. Lee et al. have reported that the chemical reduction of Ru precursor salt in the presence of ethylenediamine leads to the formation small sized Ru nanoparticles which are pretty much stable in aqueous environment. Ethylenediamine acts as a protecting agent to prevent RuNP from agglomeration [10]. When reduction of Ru precursor is carried out in liquid polyol, the size, shape and structure of Ru nanoparticles is mainly dependant on the experimental conditions. Liquid polyol function as a solvent for metal salt, reducing agent and a growth medium for Ru particles [11]. However, only few studies have emphasized the importance of electrochemical approach to control the size and morphology of Ru nanoparticles. Electrodeposition is a powerful technique to control the size, density and morphology of metal nanoparticles. During this process, the characteristics of ruthenium nanoparticles can be easily controlled according to the electrodeposition conditions [12, 13]. Most recently, we have successfully deposited gold nanoparticles on glassy carbon (GC) electrode by electrodeposition. The surface of glassy carbon was electrochemically modified to control the size, particle density and morphology of gold nanoparticles [14].

In this paper, we investigated the electrodeposition of Ru on modified GC with the view of controlling the size and density of Ru nanoparticles without using any capping agent or additives. The effect of deposition potential on the morphology of Ru nanoparticles was studied by scanning electron microscopy (SEM) of Ru deposits. The electrochemical properties of Ru nanoparticles were examined by cyclic voltammetry and linear sweep voltammetry. The activity of Ru nanoparticles for electrochemical reduction of NAD^+ to NADH was tested by three electrodes cell system.

2. EXPERIMENTAL

2.1. Reagents and apparatus

Ruthenium (III) chloride hydrate ($\text{RuCl}_3 \cdot x\text{H}_2\text{O}$; 99.9%-Ru, Strem chemicals, newburyport, MA 01950 USA) solutions were prepared in 4mM glycolic acid ($\text{HOCH}_2\text{CO}_2\text{H}$; 99% pure; Aldrich Chemical Company, Inc) at pH 3. Solution of 0.1M NaOH was used to adjust the pH of precursor ruthenium solution. The electrochemical reduction of NAD^+ (β -Nicotinamide adenine dinucleotide monohydrate; Sigma Aldrich) was carried out in 0.1M sodium phosphate buffer solution at pH 7.0

which was prepared from monosodium phosphate monohydrate and disodium phosphate heptahydrate. All the solutions were made in ultra-pure triply distilled water.

A conventional three electrode system was used for electrochemical experiments. The cell was connected to a potentiostat (IviumStat technologies, Netherland) with platinum plate (1.5cm x 1.5cm), Ag/AgCl/NaCl(sat.) reference and working electrode (1cm x 1cm). The electrochemical properties of electrodes were studied using cyclic voltammetry and linear polarization voltammetry. The particle density, distribution and surface morphology of electrodes were characterized by scanning electron microscope (NOVA NanoSEM200 - FEI Company). The products of NAD^+ reduction were analyzed by UV-Visible spectrophotometer (Cary-5000, VARIAN).

2.2. Electrochemical measurements

GC was cleaned and degreased in ethanol for 10min in ultrasonic bath, followed by rinsing with triply-distilled water three times and dried with argon gas. Electrochemical pretreatment of GC was carried out in 0.5M H_2SO_4 by potentiodynamic polarization from -1.5V to 1.5V versus Ag/AgCl at $100\text{mV}\cdot\text{s}^{-1}$ for 40 cycles. Electrodeposition of ruthenium nanoparticle was done from solution of 5mM $\text{RuCl}_3\cdot x\text{H}_2\text{O}$ in 4mM glycolic acid at pH 3 for 30 minutes. Deposition potential was adjusted as -0.28V (Electrode A), -0.32V (Electrode B), -0.36V (Electrode C) and -0.40V (Electrode D) against Ag/AgCl. After electrodeposition of Ru on GC, electrodes were annealed at 160°C for 15 hours to remove the solvent molecules attached to the Ru nanoparticles.

Electrochemical reduction of NAD^+ was studied in 0.1M sodium phosphate buffer solution at pH 7 using three electrodes cell system. The Pt electrode was separated from the solution of NAD^+ by Nafion membrane. Reduction process of 1mM NAD^+ solution (volume: 10ml) was performed at -1.2V for three hours. The solution of electrolysis was stirred at 340rpm, with continuous purging of cell with argon gas to make oxygen-free solution. All the experiments were performed at room temperature e.g. 298K.

3. RESULTS AND DISCUSSION

3.1. SEM study of Ru deposits

In order to elucidate the role of deposition potential on electrode's morphology, SEM analysis of the electrodes was carried out. Fig. 1 shows SEM images of RuNP/GC electrodes prepared at different deposition potentials. When deposition of Ru is done at -0.28 V (Electrode A), the particle density of RuNP is very low. The size distribution is approximately 90 to 110nm. Going to Electrode B, particle density increases while the particle size remains almost same. At more negative deposition potential i.e. -0.36V vs. Ag/AgCl, the morphology of electrode alters drastically. The size of RuNP decreases significantly with extremely high particle density which seems like thin film. The figure also explains that the density of the film increases when Ru is deposited at -0.40V (Electrode D). It can be inferred from the SEM results that deposition at low potentials leads to the formation of large-sized

particles while high cathodic potentials induce the formation of small-sized particles with high particle density. These observations can be explained by the fact that Ru nanoparticles have high surface energy that causes agglomeration during their deposition at low potentials as in the case of Electrode A and B. This problem can be overcome by keeping the deposition potential at -0.36V (Electrode C) that increases the active surface area of GC substrate for deposition [15]. This in turn, increases the deposition rate of Ru on GC which results in the formation of small sized RuNP with high particle density.

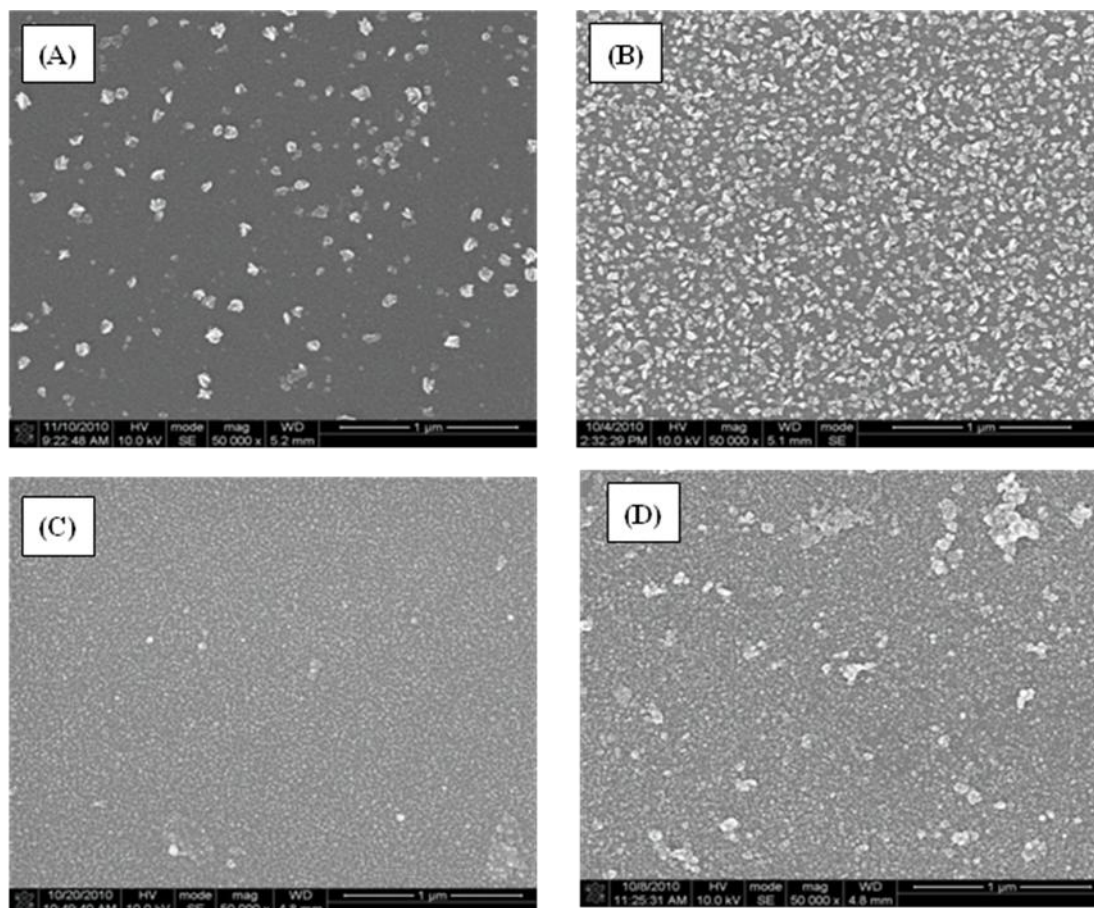


Figure 1. SEM images of Ru nanoparticles deposited on GC at different deposition potential. (A) - 0.28V , (B) -0.32V , (C) -0.36V and (D) -0.40V for 30min. Electrodeposition was performed in 4mM glycolic acid solution containing 5mM $\text{RuCl}_3 \cdot x\text{H}_2\text{O}$ at pH 3.

3.2. Electrochemical characterization

Fig. 2 displays typical cyclic voltammograms of GC and RuNP/GC electrodes in phosphate buffer of pH 7 containing 1mM of NAD^+ . Glassy carbon electrode shows a clear cathodic peak at -1.2V that is attributed to the reduction of NAD^+ ions present in solution. Previous studies [16, 17] reported that peak recorded on GC mainly leads to the formation of NAD free-radical, which involves the transfer of only one electron. When Ru is electrodeposited on GC, the electrochemical response of electrode is changed for NAD^+ reduction. Electrode A shows a reduction peak for NAD^+ reduction at

ca. -1.18V, slightly positive than GC electrode. As the particle density of Ru deposits increases for Electrode B and C (shown in Fig. 1), there is no significant change in the reduction peak position as well as in the intensity. The electrocatalytic response of these electrodes seems to be similar except for the current density.

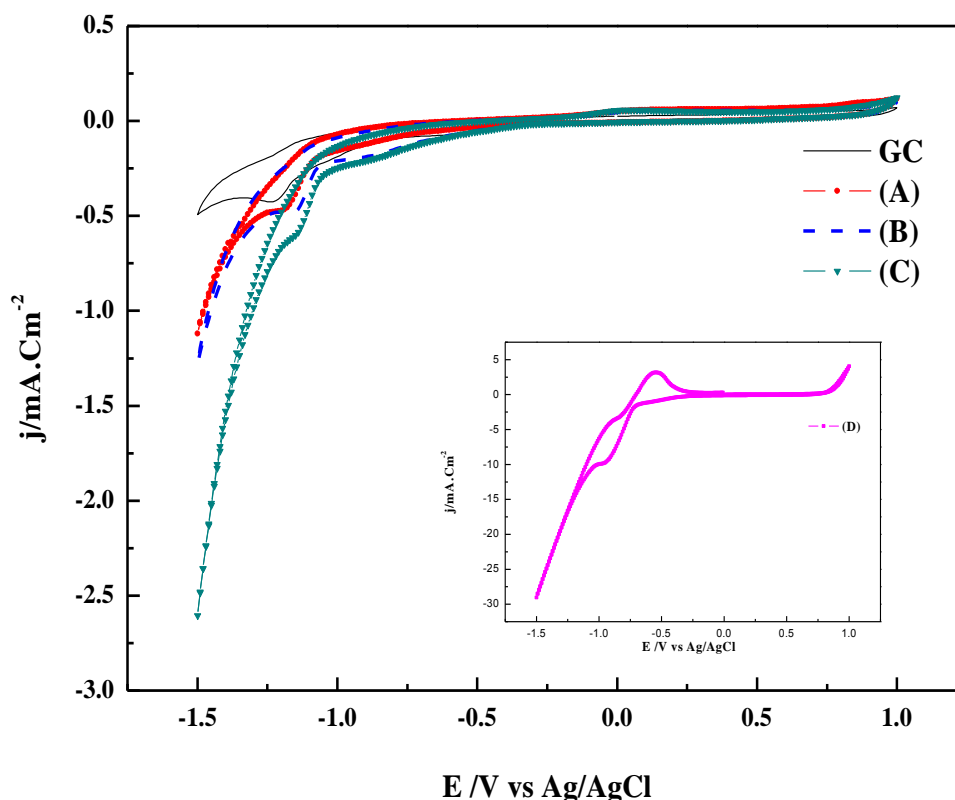


Figure 2. Cyclic voltammograms of Ru nanoparticles electrodes recorded in 0.1M sodium phosphate buffer pH 7 containing 1mM NAD^+ . (A) -0.28V, (B) -0.32V, (C) -0.36V and (D) -0.40V for 30min. Potential scan rate is $50mV.s^{-1}$. Ru film was electrodeposited from 4mM glycolic acid containing 5mM $RuCl_3 \cdot xH_2O$ at deposition potential of -0.5V for 15min.

Cyclic voltammogram of electrode D (inset to the figure) shows surprisingly different behavior. The reduction peak around -1V is a combined peak for NAD^+ reduction and hydrogen adsorption. As shown by SEM analysis, deposition of Ru nanoparticles makes film in case of Electrode D that shows different voltammetric response to NAD^+ reduction. At the starting potential of positive scan (-1.5V), a significant hydrogen evolution reaction current is observed. Along the positive sweep, there is a well defined anodic peak at ca. -0.55V which corresponds to desorption of hydrogen, adsorbed on Ru sites of the electrode [18]. The remarkably different behavior of Electrode D than others can be attributed to the different morphology of the electrode.

Since hydrogen evolution is taking place parallel to NAD^+ reduction, it is necessary to elucidate the catalytic activity of Ru nanoparticles in the background electrolyte. Fig. 3 shows a set of polarization curves recorded at various electrodes in phosphate buffer solution. Results show that GC

surface offers high hydrogen evolution overpotential which is a necessary condition for most of the reduction reactions taking place at potentials more negative than reversible H^+/H_2 couple potential [19]. The plot also demonstrates that the overpotential for hydrogen evolution changes with the change in electrode morphology (inset to the figure).

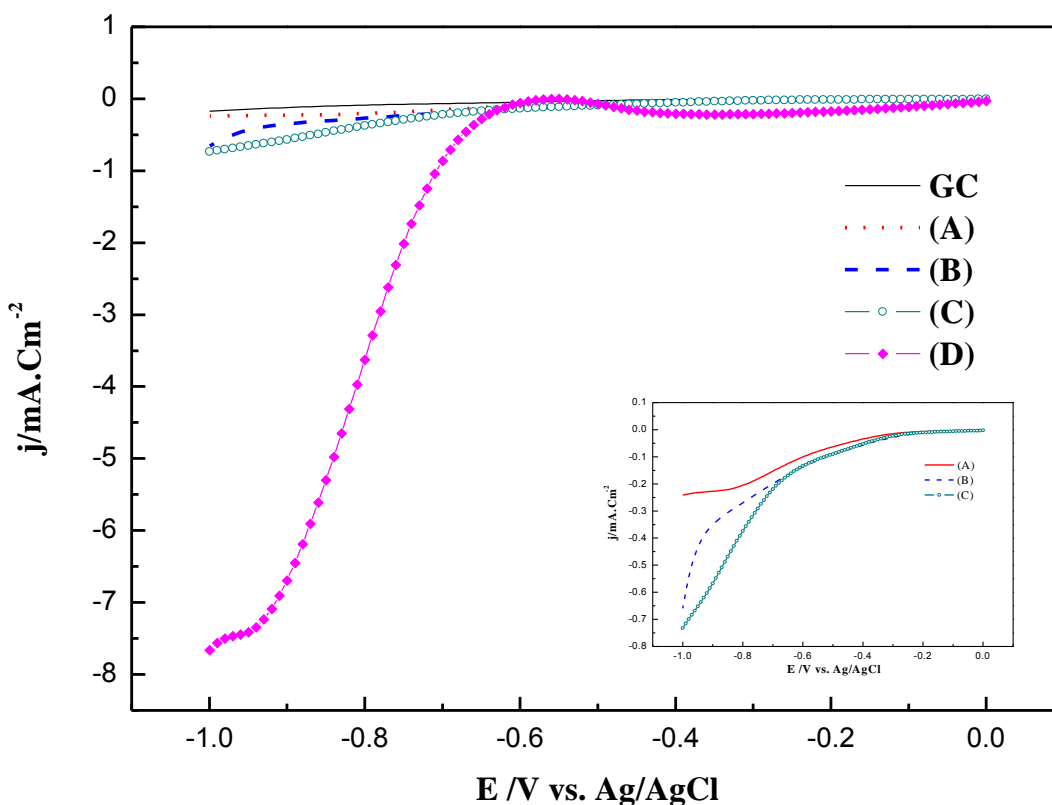


Figure 3. Linear voltammograms of electrodes recorded in 0.1M sodium phosphate buffer pH 7. (A) - 0.28V, (B) -0.32V, (C) -0.36V and (D) -0.40V for 30min. Potential scan rate is $50\text{mV}\cdot\text{s}^{-1}$. Electrodeposition was performed in 4mM glycolic acid solution containing 5mM $\text{RuCl}_3\cdot x\text{H}_2\text{O}$ at pH 3.

Electrode A does not show any significant change of overpotential for hydrogen evolution due to the small number density of Ru nanoparticles. By comparing the voltammetric curves B, C and D presented in the figure, it can be seen that the overpotential for hydrogen evolution decreases with increase in the density of Ru nanoparticles deposited on GC. However, the response of Electrode D is significantly different than other electrodes, showing extravagantly high reduction current density in the potential region of H_2 formation. The anomalous behavior of Electrode D displayed in Fig. 2 and Fig. 3 corresponds to the different morphology of RuNP, prepared at high deposition potential. As shown by SEM analysis, electroposition of Ru at -0.40V (Electrode D) leads to the formation Ru dense film that shows high activity for hydrogen evolution reaction compared to Ru nanoparticles [20].

3.3. Reduction of NAD^+ to NADH

Electrochemical reduction of NAD^+ was carried out in phosphate buffer solution pH 7 containing 1mM of NAD^+ . Previous reports [21] have shown that ruthenium has high catalytic activity for NAD^+ reduction reaction as it increases the kinetics of this process. Our study mainly deals with the effect of electrode morphology on the NAD^+ reduction reaction. As we observed in cyclic voltammetry analysis that Ru nanoparticles show a clear cathodic peak for NAD^+ reduction at ca. -1.2V, we conducted the electrochemical reduction of NAD^+ at -1.2V in phosphate buffer using GC and RuNP/GC electrodes. Fig. 4 show UV-Visible spectra of solutions after 3h reduction with the different electrodes while the inset to the figure shows NAD^+ conversion to NADH . Absorption peak at 340nm corresponds to the product, e.g. NADH [22]. Reactant NAD^+ does not show any peak around 340nm. Inset to the figure shows that GC electrode exhibits 39.3% conversion of NAD^+ to NADH . RuNP/GC electrodes show high catalytic activity with maximum conversion of 76.3% (Electrode C). Electrode D shows a sudden deterioration and only 43.4% conversion is obtained on it.

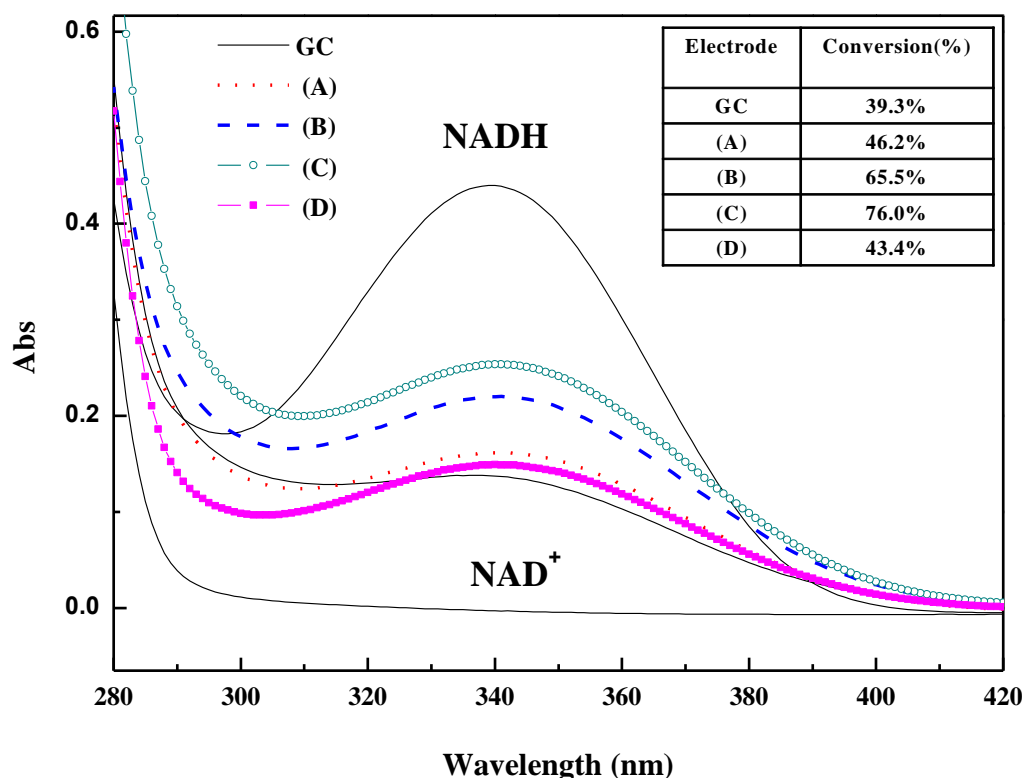


Figure 4. Absorption spectra recorded for solutions after 3h reduction of 1mM NAD^+ in 0.1M sodium phosphate buffer pH 7.0 at -1.2V with different electrodes. (A) -0.28V, (B) -0.32V, (C) -0.36V and (D) -0.40V for 30min. Ru nanoparticles were electrodeposited from 4mM glycolic acid containing 5mM $\text{RuCl}_3 \cdot x\text{H}_2\text{O}$ at pH 3.

In case of GC electrode, the yield of NADH is low due to the slow kinetics of electron transfer in NAD^+ reduction and may lead to the formation of dimer NAD_2 rather than enzymatically active

NADH as explained by Fig. 2 reference [16, 17], though it has high hydrogen evolution overpotential (Fig.3). Electrode C shows maximum conversion of NAD^+ to NADH. As depicted by SEM analysis, the size of Ru nanoparticles of Electrode C is extremely small, thereby providing high active surface area for this process. When the particle makes dense film (Electrode D), the efficiency of electrode suddenly drops down for NAD^+ reduction. Here, the reduction of NAD^+ is suppressed by hydrogen evolution reaction which is taking place side by side with NAD^+ reduction. These results are in good agreement with Fig. 2 and Fig. 3 in which Electrode D show high activity for hydrogen evolution compared to NAD^+ reduction. In order to confirm hydrogen evolution on Electrode D, we carried out pH measurement of solution after 3h reduction. The pH of solution does not change significantly during reaction using electrode A, B and C as the NAD^+ reduction is dominant. While using Electrode D as working electrode, the pH of solution increases with the progress of reaction and finally reaches up to pH 11 at the end of 3h reduction. This observation clearly explains that Ru nanoparticles in the form of Ru dense film show high activity for hydrogen evolution which is a parallel reaction with NAD^+ reduction.

4. CONCLUSION

Ru nanoparticles were successfully deposited on glassy carbon substrate by electrodeposition technique. The size and particle density of RuNP was controlled by deposition potential. The results of SEM study indicate that the size and morphology of Ru deposits is strongly dependant on deposition potential. Low potential results in the formation of large-sized Ru particles with low density while high potential leads to the formation of Ru film. Voltammetric studies show that Ru in the form of small-sized particles exhibit low overpotential for NAD^+ reduction. UV-Visible measurements of NAD^+ reduction conclude that Ru nanoparticles that are obtained at -0.36V deposition potential exhibit significantly high electrocatalytic activity for electrochemical reduction of NAD^+ .

ACKNOWLEDGMENT

This research was supported by the Converging Research Center Program through the National Research Foundation of Korea (NRF) funded by the Ministry of Education, Science and Technology.

References

1. Y.H. Qi, P. Desjardins, X.S. Meng, Z.Y. Wang, *Optical Materials*. 21 (2003) 255.
2. S.H. Joo, J.Y. Park, J.R. Renzas, D.R. Butcher, W. Huang, G.A. Somorjai, *Nano Letters*, 10 (2010) 2709.
3. L. Yao, T. Shi, Y. Li, J. Zhao, W. Ji, C.T. Au, *Catalysis Today*, In Press, Corrected Proof.
4. L. Zhang, Z. Xu, S. Dong, *Analytica Chimica Acta*. 575 (2006) 52.
5. Z. Jia, T.I. Ren, T.Z. Liu, H. Hu, Z.G. Zhang, D. Xie, L.T. Liu, *Mat. Sci. Eng: B*, 138 (2007) 219.
6. F. Man, S. Omanovic, *J. Electroanal. Chem.* 568 (2004) 301.
7. W.A. van der Donk, H. Zhao, *Curr. Opin. Biotech.* 14 (2003) 421.

8. C. Pan, K. Pelzer, K. Philippot, B. Chaudret, F. Dassenoy, P. Lecante, M.J. Casanove, *J. Am. Chem. Soc.* 123 (2001) 7584.
9. S. Chen, R.W. Murray, *Langmuir*. 15 (1998) 682.
10. J.Y. Lee, J. Yang, T.C. Deivaraj, H.P. Too, *J. Colloid. Interfac. Sci.* 268 (2003) 77.
11. G. Viau, R. Brayner, L. Poul, N. Chakroune, E. Lacaze, F. Fievet-Vincent, F. Fievet, *Chem. Mat.* 15 (2002) 486.
12. C. Thambidurai, Y.G. Kim, J.L. Stickney, *Electrochim. Acta.* 53 (2008) 6157.
13. O. Azzaroni, P.L. Schilardi, R.C. Salvarezza, *Electrochimica Acta*, 48 (2003) 3107-3114.
14. G. Rahman, J.Y. Lim, K.D. Jung, O.S. Joo, *Electrochem. Commun.* 12 (2010) 1371.
15. M.O. Finot, G.D. Braybrook, M.T. McDermott, *J. Electroanal. Chem.* 466 (1999) 234.
16. M. Studnickova, H.P. Klukanova, J. Turanek, J. Kovar, *J. Electroanal. Chem. Interfac. Electrochem.* 252 (1988) 383.
17. P.J. Elving, W.T. Bresnahan, J. Moiroux, Z. Samec, *Bioelectrochem. Bioenerg.* 9 (1982) 365.
18. Vuorilehto, S. Lutz, C. Wandrey, *Bioelectrochem.* 65 (2004) 1.
19. A.Koca, *Int. J. Hyd. Energy.* 34 (2009) 2107.
20. J.M. Jaksic, N.M. Ristic, N.V. Krstajic, M.M. Jaksic, *Int. J. Hyd. Energy.* 23 (1998) 1121.
21. A.Azem, F. Man, S. Omanovic, *J. Mol. Catal. A: Chemical* 219 (2004) 283.
22. L. Zhang, Y. Li, L. Zhang, D.W. Li, D. Karpuzov, Y.T. Long, *Int. J. Electrochem. Sci.* 6 (2011) 819.